Sea-surface aerodynamic roughness

L. Mahrt and Dean Vickers
College of Oceanic and Atmospheric Sciences, Oregon State University, Corvallis, Oregon, USA

Paul Frederickson and Ken Davidson
Naval Postgraduate School, Monterey, California, USA

Ann-Sofi Smedman
Department of Meteorology, University of Uppsala, Uppsala, Sweden

Received 11 March 2002; revised 30 October 2002; accepted 6 March 2003; published 3 June 2003.

[1] This study surveys and evaluates similarity theory for estimating the sea-surface drag coefficient with the bulk aerodynamic method. The most commonly used formulations of the aerodynamic roughness length, required by similarity theory, are examined using data sets from four different field programs. These relationships include the Charnock formulation and the wave age modified Charnock relationship. The goal is to assess the overall performance of simple formulations of the roughness length including cases where the Charnock formulation is not expected to apply, and to assess the errors resulting from application of the Charnock formulation to all conditions, as is done in many numerical models where an explicit wave model cannot be accommodated. This examination indicates that spurious self-correlation explains more variance than actual physical relationships, even after eliminating weak wind cases. Frequent cases of anomalously low stress and very small values of the Charnock coefficient further reduce the usefulness of this formulation for the present data sets. Causes of the frequent very small values of the Charnock coefficient are briefly investigated. *INDEX TERMS:* 0312 Atmospheric Composition and Structure: Air/sea constituent fluxes (3339, 4504); 3339 Meteorology and Atmospheric Dynamics: Ocean/atmosphere interactions (0312, 4504); 4504 Oceanography: Physical: Air/sea interactions (0312); 3307 Meteorology and Atmospheric Dynamics: Boundary layer processes; *KEYWORDS:* roughness length, aerodynamic roughness length, Charnock formulation, sea-surface stress, wave state, Monin-Obukhov similarity

Citation: Mahrt, L., D. Vickers, P. Frederickson, K. Davidson, and A.-S. Smedman, Sea-surface aerodynamic roughness, *J. Geophys. Res.*, *108*(C6), 3171, doi:10.1029/2002JC001383, 2003.

1. Introduction

[2] The surface stress over the sea is normally formulated in terms of a drag coefficient based on the aerodynamic roughness length for momentum for the sea surface (hereinafter referred to as the roughness length) and the stability functions for Monin-Obukhov similarity theory [e.g., *Donelan*, 1990]. While there are common conditions where Monin-Obukhov similarity theory does not apply, the fact that the sea surface is a moving surface, by itself, does not preclude application of Monin-Obukhov similarity theory in the surface layer. Monin-Obukhov similarity theory often approximates the behavior of the turbulence energy budget [*Edson and Fairall*, 1998; *Wilczak et al.*, 1999] and flux-gradient relationship [*Vickers and Mahrt*, 1999] as long as the observations are in the surface layer, above the wave boundary layer [e.g., *Hare et al.*, 1997]. With weak winds and swell, a surface layer where Monin-Obukhov similarity theory is valid cannot be identified [*Smedman et al.*, 1999; *Grachev and Fairall*, 2001].

[3] After reviewing a generalized similarity theory applied to the sea surface (section 2), section 3 discusses different formulations of the roughness length. Data sets for evaluation of parameterization of the roughness length are described in section 4. The strong role of self-correlation in the parameterization schemes is studied in section 5. The large variability of the Charnock coefficient between data sets and wind speed and wave age regimes is studied in section 6. Our goal is to assess the errors resulting from application of the Charnock relationship to a wide variety of conditions, as is done in most regional and large-scale models, cannot accommodate the complexity and computer time required for a wave model. To construct such an assessment, we will not remove common cases of swell or other conditions where the Charnock relationship is not expected to apply.

2. General Similarity Theory

[4] Formulation of momentum transfer in the atmosphere adjacent to the surface is often expressed in terms of an

Copyright 2003 by the American Geophysical Union.
0148-0227/03/2002JC001383$09.00

inverse flux-gradient relationship, referred to as the nondimensional shear,

$$\phi_m \equiv \frac{\kappa z}{u_*}\frac{\partial u}{\partial z} = f\left(z/L, Re_*, z/\lambda, z/h, G\right), \quad (1)$$

where the far right-hand side includes suspected possible influences on the flux-gradient relationship for stationary homogeneous flow. Here, Re_* is the roughness Reynolds number, λ is a length scale for the waves, h is the boundary-layer depth, and G is a functional dependence on additional influences, all discussed in this section. L is the Obukhov length, which represents the influence of atmospheric stability on generation or inhibition of turbulence near the surface. If only the first argument on the right-hand side is retained, equation (1) reduces to Monin-Obukhov similarity theory.

[5] A more practical formulation for the surface stress is traditionally constructed by solving for the surface friction velocity and vertical integrating the nondimensional gradient from the observation level to near the surface, in which case the drag coefficient is formulated as

$$C_d \equiv \frac{u_*^2}{U^2} = F\left(\ln\frac{z}{z_o}, z/L, Re_*, z/h, z/\lambda, G\right), \quad (2)$$

where U is the wind speed computed from the time-averaged wind components at the observational level. The lower limit of integration is z_o, the aerodynamic surface roughness length. This is the level at which the wind predicted by equation (2) with only z/L and ln (z/z_o) as arguments, vanishes when extrapolating toward the surface. The roughness length has not been rigorously formulated for cases where other arguments (Re_*, z/h, z/λ, G) become important, although additional influences are sometimes "added" to traditional formulations, discussed below.

[6] The near-surface flow can be divided into the wave boundary layer adjacent to the surface and the overlying surface layer. In the wave boundary layer [e.g., *Hare et al.*, 1997], the flux-gradient relationship depends on length scales associated with the geometry of the surface. The influence of the wave length scales become unimportant in the overlying surface layer where Monin-Obukhov similarity theory may be valid. The wave length scale, represented by λ in equation (1), is sometimes chosen as the wavelength or wave height of the dominant waves or some scale derived from the wave spectra. With concurrent wind-driven waves and swell, the statistical analysis of *Rieder and Smith* [1998] suggests that the stress vector is rotated from the wind vector by any swell that propagates in a direction significantly different from the wind direction, invalidating Monin-Obukhov similarity theory. *Grachev and Fairall* [2001] found that the influence of swell on the surface stress was particularly large for weak wind conditions, causing the wind and stress directions to be different.

[7] The roughness Reynolds number, Re_*, represents the influence of smooth flow viscous effects [e.g., *Brutsaert*, 1982], which may become important in weak wind cases. Related influences include surface tension and surfactants, which are most likely to be important in weak wind conditions. As a result of the multitude of complications for weak wind conditions, the data analysis in section 5 will first be conducted without weak wind conditions.

[8] With thin atmospheric boundary layers, the influence of the boundary-layer depth, h, on the flux-gradient relationship may extend downward to the surface. For example, *Mahrt et al.* [1998] found that the shallow depth of the internal boundary layer in offshore flow over warm water restricted the development of large convective eddies, causing the transfer coefficient to be smaller than that predicted by Monin-Obukhov similarity theory. This argument was extended to the nondimensional shear by *Vickers and Mahrt* [1999].

[9] The effect of the stability is particularly strong in near-collapse of the turbulence in warm air advection over cooler water [*Smedman et al.*, 1997a, 1997b; *Mahrt et al.*, 2001a, 2001b] where Monin-Obukhov theory may not be applicable, or applicable only in a thin surface layer below traditional observational levels. If the influence of the boundary layer depth extends down to the wave boundary layer, then a surface layer where Monin-Obukhov theory applies, does not exist.

[10] Other influences, not explicitly represented above, may become important in special situations and are collectively included in the argument G. Such influences include nonstationarity and baroclinicity (thermal wind) [*Geernaert*, 1996]. Advection of stronger turbulence from land can also alter the flux-gradient relationship immediately downstream from the coast [*Vickers et al.*, 2001]. With shear instability above thin stable boundary layers, turbulence energy may be transported downward toward the surface and alter the flux-gradient relationship near the surface [*Mahrt et al.*, 2001a, 2001b].

[11] Sorting out the various influences on the flux-gradient relationship is not normally possible with existing data, and progress has been made only when several of the above influences can be neglected. The most notable case is Monin-Obukhov similarity theory where all of the above arguments on the right-hand side of equation (2) can be neglected except z/L and ln z/z_o. Then the drag coefficient can be formulated with Monin-Obukhov similarity theory as

$$C_d = \frac{u_*^2}{U^2} = \left[\frac{\kappa}{\ln(z/z_o) - \psi_m}\right]^2. \quad (3)$$

The stability function, ψ_m, must be specified as a function of z/L. We choose the formulations from *Paulson* [1970] for the unstable case and *Dyer* [1974] for the stable case. Given observed fluxes and mean wind, the roughness length can be computed from equation (3). The roughness length computed from observations can be contaminated by either failure of Monin-Obukhov similarity theory due to influences discussed above or inaccurate specification of ψ_m, as might be expected in very stable conditions. In these cases, the relationship between the estimated roughness length and actual roughness of the waves becomes obscure [*Sun et al.*, 2001]. Numerical models are required to apply Monin-Obukhov similarity to all situations because suitable alternatives do not exist.

[12] In cases where no information is available on wave state, the roughness length is often formulated in terms of the Charnock formulation [*Charnock*, 1955] with constant coefficient, as is applied in the commonly used TOGA

COARE algorithm [*Fairall et al.*, 1996] as well as numerous other models. Is it possible to improve upon this scheme without any information on wave state?

3. Formulation of the Aerodynamic Roughness Length

[13] The roughness length is computed from equation (3) using the observed fluxes and wind speed and stability functions. The computed roughness length assumes that the stability functions are correct, the measured quantities are correct and that they are measured in the surface layer, above the wave boundary layer. Otherwise, the physical interpretation of the roughness length becomes vague since it must compensate for inadequacies in the data or for all of the influences not included in Monin-Obukhov similarity theory; that is, the last four arguments on the right-hand side of equation (2).

[14] A goal of this study is to evaluate the applicability of the Charnock relationship. The Charnock formulation is a common parameterization of the aerodynamic roughness length over the water, which does not explicitly incorporate information on wave state. This relationship has been applied to snow and ice surfaces as well [*Andreas and Claffey*, 1995]. It is written as

$$z_o = \alpha \frac{u_*^2}{g}, \tag{4}$$

where α is the Charnock coefficient, often referred to as a nondimensional roughness length. This formulation assumes that the influence of wave state on the roughness length is represented by the surface stress.

[15] For neutral conditions (no buoyancy flux), one can combine equation (3) with the Charnock parameterization to obtain

$$\ln\left(\frac{z}{z_o}\right)^2 = \frac{\alpha\kappa^2}{g} U^2. \tag{5}$$

Since the left-hand side of equation (5) is an increasing function of the roughness length, this relationship predicts that the roughness length increases with wind speed. Since this increase is counter to observational tendencies for weak wind conditions, the Charnock relationship with constant coefficient cannot be used for weak wind conditions, even as a first approximation (section 6).

[16] Sometimes the roughness length is defined in terms of the Charnock term (equation (4)) and a smooth flow term in which case the Charnock coefficient is computed as [e.g., *Fairall et al.*, 1996]

$$\alpha_s = \left(z_o - 0.11 \frac{\nu}{u_*}\right) \frac{g}{u_*^2}. \tag{6}$$

For weak wind speeds or small roughness Reynolds number, this value of the Charnock coefficient can be substantially less than the traditional value (equation (3)). Except when specified otherwise, we will use the original definition of the Charnock coefficient (equation (4)).

[17] The Charnock relationship is often generalized by introducing a dependence on wave age as given by *Toba and Koga* [1986], *Maat et al.* [1991], *Donelan* [1990] and *Smith et al.* [1992]. This dependence can be expressed as

$$\alpha = K\left(\frac{u_*}{C_p}\right)^p, \tag{7}$$

where K and p are empirical parameters and C_p is the phase speed of the dominant waves. Recall that dependence of the roughness length on wave state is compatible with Monin-Obukhov similarity theory while direct dependence of the flux-gradient relationship on wave scales (such as λ) is not compatible. Recently, *Drennan et al.* [2003] analyzed data from five field programs and found overall values of K = 1.59 and p = 1.67. Incorporating this expression for the Charnock coefficient into equation (4),

$$z_o = K\left(\frac{u_*^2}{g}\right)\left(\frac{u_*}{C_p}\right)^p, \tag{8}$$

where p = 1.

[18] *Donelan* [1990] scaled the roughness length with the rms wave height and related it to inverse wave age, such that

$$\frac{z_o}{\sigma} = K\left(\frac{u_*}{C_p}\right)^p. \tag{9}$$

Drennan et al. [2003] found best fit values of K = 13.3 and p = 3.4. These relationships will be evaluated in section 5.

4. Data Sets and Flux Computation

[19] This study analyzes offshore tower and buoy data collected during six different field programs, each with unique geographical characteristics. The Ris Air Sea Experiment (RASEX) is described by *Barthelmie et al.* [1994] and *Højstrup et al.* [1995]. In this study, we analyze observations taken at the sea mast west tower, located 2 km off the northwestern coast of the island of Lolland, Denmark, in 4 m of water, for the intensive observing period 3 October through 8 November 1994. The variation in mean water depth due to tides is only about 0.3 m. Local off-shore (southeasterly) flow is characterized by a sea fetch ranging between 2 km and 5 km. Sea fetch is the distance from land to the sea mast following the wind. Onshore flow has a sea fetch between 15 km and 25 km as it travels across an inland sea, and is still potentially fetch-limited in terms of wave age. Swell is less important compared to the other data sets. Fetch is the distance along the flow from the coast to the sea mast. Water depths for the longer fetches range from 4 m to 20 m. The nearby land surface is relatively flat. For additional characteristics of the instrumentation and flow regimes, see *Mahrt et al.* [2001b, and references therein]. These data sets have been quality controlled using procedures similar to those of *Vickers and Mahrt* [1997a]. In contrast to *Vickers and Mahrt* [1997b], we analyze the 6-m eddy correlation data instead of the 10-m data since the 6-m level is more suitable for thin stable boundary layers.

[20] The largest data set analyzed here was collected from a 30-m tower at the tip of a small very flat island (Östergarnsholm) approximately 4 km east of Gotland, Sweden.

The footprint of the tower is over water with flow from the southerly sector. The bathymetry south of the island leads to minimal shoaling. Here we analyze eddy correlation data collected at the 8-m level using a Gill Solent 101R2 sonic anemometer and wave data collected from a directional wave-rider buoy deployed approximately 4 km south of the site. These data contain a number of cases where the momentum flux was upward from the sea to the atmosphere. These cases are neglected in this study. Additional description of the instrumentation is detailed by *Smedman et al.* [1999].

[21] We also analyze fluxes acquired by the Naval Postgraduate School's "flux" buoy during two experiments conducted off the U.S. east coast. Both data sets are at approximately 5.25 m above mean sea level. During the first experiment, conducted in February–March of 1999, the buoy was located 10.5 km offshore of Duck, North Carolina, in 23 m of water. In the second experiment, conducted in May–June 2000, the buoy was moored 13 km off Wallops Island, Virginia, in water 14 m deep. Unlike the two data sets previously described, which were obtained from stable towers, the NPS buoy measurements required motion corrections to remove wave motion-induced contamination from the observed wind data before eddy-correlation fluxes could be computed. High-frequency 3-D wind and sonic temperature data were obtained from a Gill Instruments Model 1012/R3 ultrasonic anemometer mounted 5.25 m above the water surface. The buoy 3-D angular and linear motion data, used to perform motion corrections and to compute wave statistics, were obtained from a Systron-Donner MotionPak located within the buoy hull. The significant wave height was computed by summing the variance spectra for vertical displacement and multiplying by 4. Further information on the NPS flux buoy instrumentation and data analysis procedures is given by *Frederickson and Davidson* [2003].

[22] After restrictions in subsection 4.1, the RASEX data set consists of 286 1-hour records, the NPS Wallops Island data set consists of 697 74-min records, the NPS Duck data set consists of 313 48-min records, and the Östergarnsholm data set consists of 1142 1-hour records.

[23] For auxiliary analyses, additional data are extracted from *Smith* [1980] for open ocean conditions and SWADE data from Lake Ontario [*Donelan et al.*, 1997]. The data from Smith contain no cases of winds less than 4 m s^{-1} and are therefore listed only in Table 1. Since the SWADE data set is relatively small, we report values only for all wind speeds.

4.1. Data Subsets

[24] The influence of advection of turbulence from land appears to be confined primarily to the first 5 km downstream from the shore depending on wind speed and the upstream turbulence over land [*Vickers et al.*, 2001]. We require that the fetch is greater than 10 km. Because we pose no restrictions, such as minimum wind speed or flux magnitude, and because of the very large data sets, extreme values of the roughness lengths occur for some of the records. These extreme values can substantially influence attempts to fit the data with a model or compute bin-averaged values for different intervals of an independent variable. Therefore we eliminate 5% of the outliers on both extremes of the frequency distribution of the roughness length.

Table 1. Fraction of Variance Explained by Various Models for the Aerodynamic Roughness Length[a]

	Char		Hyper		W.age		W.height	
Data Set	Orig	Sim	Orig	Sim	Orig	Sim	Orig	Sim
NPS-Duck	0.81	0.58	0.93	0.89	0.80	0.56	0.72	0.42
NPS-Wallops Island	0.67	0.55	0.85	0.88	0.62	0.54	0.49	0.43
Öster.-8 m	0.58	0.60	0.89	0.94	0.57	0.57	0.46	0.33
RASEX-6 m	0.35	0.55	0.79	0.94	0.36	0.53	0.31	0.35
Smith (1980)	0.76	0.70	0.92	0.96	-	-	-	-

[a]The Charnock formulation $z_o = \alpha u_*^2/g$ (char), the hyper model $z_o = (u_*^9/U^7)/g$ (hyper, equation (10)), the wave age dependent model $z_o = (u_*/c_p)\alpha u_*^2/g$ (w.age, equation (7)) and the wave height dependent model $z_o = \sigma_h(u_*/c_p)^3$ (w.height, equation (9)). Orig indicates the variance explained using the data sets listed in the first column. Sim indicates the variance explained after randomizing the data as described in section 4. Weak winds ($U < 4$ m s^{-1}) are excluded.

4.2. Averaging

[25] Partly because of random flux errors, the relationship between the roughness length and other variables is generally characterized by large scatter. Averaging the roughness lengths for a given interval of the independent variable can be strongly influenced by extreme values of the roughness length not excluded by the above criteria. With roughness lengths approaching zero, the log of the roughness length assumes very large negative values. As a result, logarithmically averaging roughness lengths lead to substantially smaller values of the roughness length compared to linearly averaging the roughness lengths. The frequency distribution of the log of the roughness lengths is approximately normal whereas the frequency distribution of the roughness length itself is strongly skewed toward positive values. In the latter case, averaging is not as well posed compared to normal distributions. An additional argument for logarithmic averaging is that the drag coefficient and stress depend on the natural logarithm of the roughness length. In subsequent sections, we will show results from both linear and logarithmic averaging.

4.3. Self-Correlation

[26] In general, the formulation of the roughness length in terms of other variables involving the friction velocity, heat flux, and wind speed is influenced by self-correlation. Unless the variance explained by this self-correlation is estimated, it is not possible to determine from data if the formulation represents true intervariable physical relationships. For example, the Charnock relationship relates the roughness length to the surface friction velocity; however, the roughness length is by definition a function of the surface friction velocity through the Monin-Obukhov relationship for the surface stress (equation (3)). As a result, *Smith et al.* [1996] dismisses the Charnock relationship as a physically useful expression.

[27] As one measure of the spurious self-correlation, we randomly redistribute the observed values of the friction velocity, heat flux, wind speed, wave phase speed, and significant wave height. This process is carried out by assigning a record number to each of the N records for a given data set. The friction velocity for the first new random record is extracted from a record number chosen at random.

This process is repeated independently for each variable until a new random record is determined. This process is repeated until a set of N new random records are constructed. For the N new random records, we compute the roughness length from the randomized data for each of the N records and then compute the variance explained by the various roughness-length formulations. This entire process is repeated for one thousand realizations and then the thousand values of the variance explained is averaged over all of the realizations. The procedure is applied to each of the data sets.

[28] The variance explained by the original data less the variance explained by the randomized data is an estimate of the true physical variance explained. Since the randomized data may lead to very large absolute values of z/L, we impose the restriction $abs(z/L) < 2$ for both the original and randomized data. This restriction is applied only for this side study of self-correlation. The variance explained is based on the logarithm of the roughness length since the logarithm of the roughness length appears in the similarity prediction of the stress.

[29] We have also examined the self-correlation by randomly specifying the values of wind speed and heat and momentum fluxes according to a Gaussian distribution. While generally supporting results from the above ''random redistribution'' approach, the results based on the Gaussian noise approach depend on the assumption of normality. In this study, we report only results from the random redistribution approach.

5. Aerodynamic Roughness Length and Charnock Coefficient

[30] Even with near neutral conditions and large sea fetches, the Charnock coefficient for individual records varies by orders of magnitude partly due to the influence of wave age as well as random error. On the basis of studies in the literature as well as the present data sets, the Charnock coefficient generally (1) decreases with wave age, (2) increases at weak wind speeds with large scatter, (3) is large for short sea fetch conditions (excluded from the present analysis) partly due to small wave age and advection of turbulence from land, and (4) is sometimes exceptionally small for stable conditions associated with warm air advection.

[31] We temporarily remove weak wind cases ($U < 4$ m s^{-1}) because the Charnock formulation is particularly poor for such conditions (section 3). This condition removes many, but not all, of the ultra-smooth cases. Weak-wind cases will be restored at the end of this section. Except for large friction velocities, the logarithmic ''average'' value of the roughness length corresponds to a Charnock coefficient, which is smaller than in most previous data sets, partly because of the exclusion of weak wind cases and occurrence of a large number of records with wind following swell, discussed further in section 6. The linear average of the roughness length corresponds to values of the Charnock coefficient, which are closer to previously published estimates (Figure 1). However, the average of the logarithm of the roughness lengths is much closer to a normal distribution and more suitable to averaging. For the combined data sets excluding the weak wind cases, the roughness length

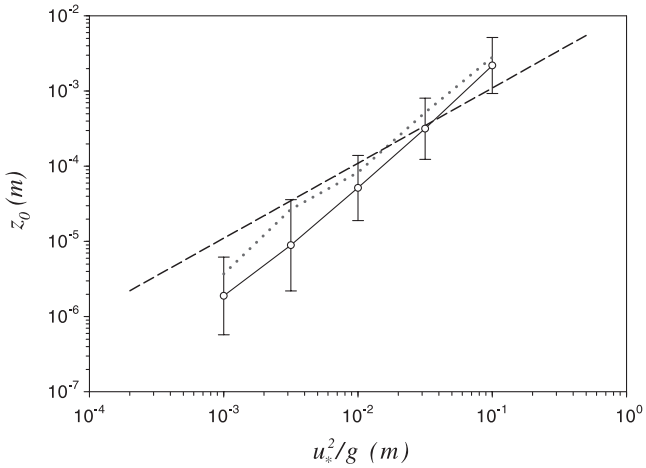


Figure 1. Dependence of the roughness length on u_*^2/g for all of the data sets combined using logarithmic averaging (solid line), excluding weak wind cases. The dotted line represents linear averaging. The dashed line is the Charnock prediction with $\alpha = 0.011$. The error bars indicate plus/minus 1 standard deviation. Standard errors would be extremely small because of the very large data set and would not be visible on the plot.

increases with u_*^2/g faster than linearly (Figure 1) so that corresponding Charnock coefficient increases with u_*^2/g.

[32] Large scatter occurs in spite of self-correlation between the roughness length and friction velocity. This self-correlation is guaranteed by the definition of the roughness length (equation (3)) and the definition of the drag coefficient. To investigate this self-correlation, we randomly rearranged the observed values, as described in section 4 and then computed the roughness length from the randomized data using equation (3). On the basis of these estimates, the physical variance explained (original variance minus that due to self-correlation) exceeds 20% only for the NPS-Duck data set (Table 1). Consequently, the variance explained by the Charnock relationship is usually dominated by spurious self-correlation. If the underlying physical correlation is of opposite sign to that introduced by self correlation, then the physical variance explained is negative and therefore not a true variance.

[33] The Charnock coefficient increases with friction velocity probably because of the exponential dependence of the roughness length on u_*, embedded in the similarity relationship (equation (3)) along with dependencies on wind speed and stability z/L. For neutral conditions, the roughness length and friction velocity are uniquely related for a given wind speed and observational height (equation (3)). As an instructive example, we capitalize on this self-correlation and construct a two-parameter hypergeneralization of the Charnock relationship of the form

$$\alpha \equiv \frac{z_o g}{u_*^2} = K^* \left(\frac{u_*}{U}\right)^{p*}, \tag{10}$$

which allows for a higher-order dependence of the roughness length on the friction velocity compared to the Charnock relationship. The constant coefficient K^* does not influence the variance explained. Rather, large values of

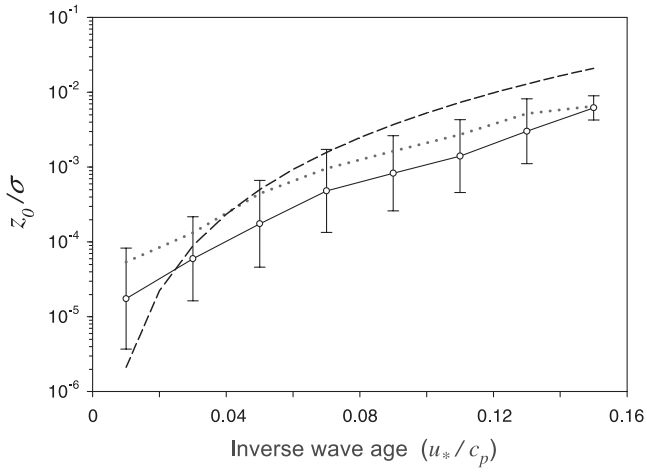


Figure 2. Dependence of the scaled roughness length on inverse wave age for all of the data sets, excluding weak wind cases. The dashed line presents the model of *Drennan et al.* [2003]. The dotted line represents linear averaging.

the exponent p^* provide the best fit. The second column in Table 1 lists the variance explained for $p^* = 7$. This relationship explains substantially more variance than the original Charnock relationship, approximately 90% (Table 1). However, within the error of estimating the self-correlation, the success of this model is due almost exclusively to self-correlation. This relationship simply captures even more spurious self-correlation than the original Charnock relationship.

[34] One must also exercise care in interpreting the physical significance of additional parameters, which increase the order of the dependence of the roughness length on the friction velocity. For example, relating the roughness length to inverse wave age (equation (8)) increases the dependence of the roughness length on the friction velocity by order p compared to the original Charnock formulation. For the wave-age dependent model ($p = 1$, column 3, Table 1), neither the total variance explained nor the variance explained by self-correlation increases significantly compared to the case of constant Charnock coefficient, even though relating the roughness length to inverse wave age is physically motivated by the expectation that growing young waves require more stress input than mature waves for a given wave amplitude.

[35] The relative unimportance of wave age as an additional variable contrasts with *Vickers and Mahrt* [1997b], who found that the drag coefficient in RASEX, reduced to neutral, was significantly influenced by wave age. However, in their study, more stringent restrictions were placed on the allowed magnitude of z/L and cases with large random flux error were eliminated. These conditions reduce the scatter but create a bias in that they preferentially eliminate weak wind cases. They also included cases with sea fetch less than 10 km where the wave-age effect is particularly strong. *Johnson et al.* [1998] show that the dependence of the Charnock coefficient on wave age becomes evident only when combining a variety of data sets in order to represent a sufficiently wide range of wave age.

[36] Relating the roughness length scaled by the rms wave height to the inverse wave age (equation (9)) explains substantially more physical variance only for the NPS-Duck data (fourth column, Table 1). On the basis of bin-averaged values for intervals of the inverse wave age, this model agrees with the trend found in the observations both in terms of the roughness length (Figure 2) and the Charnock coefficient (not shown). The magnitude of the scaled roughness length is generally smaller than that predicted by the model of *Drennan et al.* [2003], partly for reasons discussed above. On the other hand, using completely random data (section 4), the bin-averaged nondimensional roughness length follows equation (9) reasonably well, although with a stronger dependence on inverse wave age, underscoring the role of self-correlation (also not shown).

[37] Large self-correlation can be partly due to greater variation of the friction velocity compared to the wave phase speed. *Drennan et al.* [2003] reduces the impact of spurious self-correlation inherent with relating the roughness length to wave age, by seeking data with a wide range of wave phase velocities. Like *Drennan et al.* [2003], we examine subsets of the data where the friction velocity is confined to a narrow interval, ensuring that the variation of wave age for the subset is due primarily to variation of wave phase speed. We found that partitioning data into intervals of friction velocity seriously reduced the variance explained by equation (9); that is, equation (9) is affected by significant self-correlation for our data. Some of our data are significantly influenced by swell in spite of removal of weak wind cases. *Drennan et al.* [2003] carefully removed cases of significant swell.

[38] If we include weak-wind cases, both the total variance explained and the variance explained due to self-correlation are substantially less for most of the data sets and models in this section (Table 2). For specification of constant Charnock coefficient, the total variance explained may be significantly less than that due to self-correlation. That is, for weak wind speeds, the Charnock formulation produces the wrong sign in the change of roughness length with wind speed and actually reduces the variance explained below the self-correlation value.

6. Ultra-Smooth Conditions

[39] Often the roughness length computed from observations is smaller than that due to the smooth flow term, corresponding to ultra-smooth conditions [*Donelan*, 1990]. For three of the four data sets, ultra-smooth cases comprise a significant fraction of the cases; 38% for the NPS-Duck data, 49% for the Wallops Island data, and 42% for the Östergarnsholm data. Only for the RASEX data are ultra-smooth conditions rare and the Charnock coefficient averages near the traditional value of 0.01. The RASEX data

Table 2. Same as Table 1 Except That Weak Winds are Included

	Char		Hyper		W.age		W.height	
Data Set	Orig	Sim	Orig	Sim	Orig	Sim	Orig	Sim
NPS-Duck	0.67	0.55	0.91	0.88	0.66	0.53	0.62	0.40
NPS-Wallops Island	0.17	0.43	0.55	0.85	0.16	0.42	0.14	0.35
Öster.-8 m	0.38	0.51	0.82	0.92	0.37	0.49	0.29	0.31
RASEX-6 m	0.25	0.52	0.67	0.92	0.24	0.51	0.20	0.37
SWADE	0.47	0.58	0.90	0.92				
SWADE-pure	0.85	0.69	0.98	0.97				

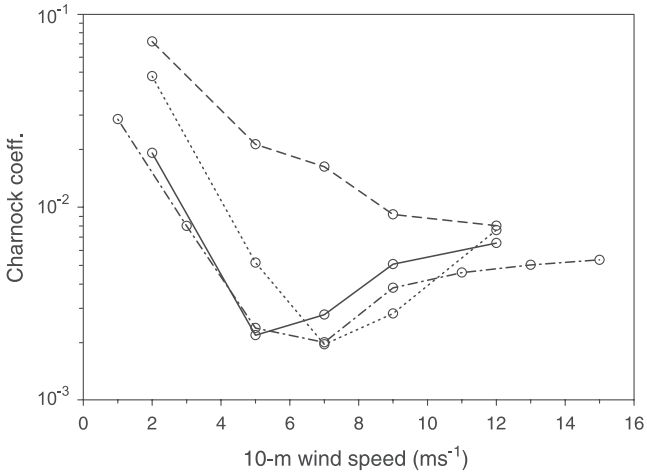


Figure 3. Dependence of the Charnock coefficient on wind speed for RASEX data (dashed line), Wallops Island data (dotted line), NPS-DUCK data (solid line), and Östergarnsholm data (dash-dotted line) for logarithmic averaging. Values are several times larger for linear averaging.

correspond to an inland sea and is the only data set with minimal swell.

[40] *Donelan* [1990, p. 256] suggests that small differences between the wind and swell phase velocities could contribute to ultra-smooth conditions. Wind waves are thought to be suppressed with wind following the swell [*Phillips and Banner*, 1974; *Mitsuyasu and Kusaba*, 1996]. The stress can decrease to arbitrarily small values, vanish, and even reverse sign, corresponding to upward momentum flux from the sea to the atmosphere [*Smedman et al.*, 1994; *Grachev and Fairall*, 2001, and references therein]. When the swell-driven upward momentum flux approximately balances the downward wind driven momentum flux, the total stress is very small. For the data from *Grachev and Fairall* [2001], such conditions corresponded to winds between 1 and 2 m s^{-1}, although some influence of swell appeared to extend to stronger wind speeds.

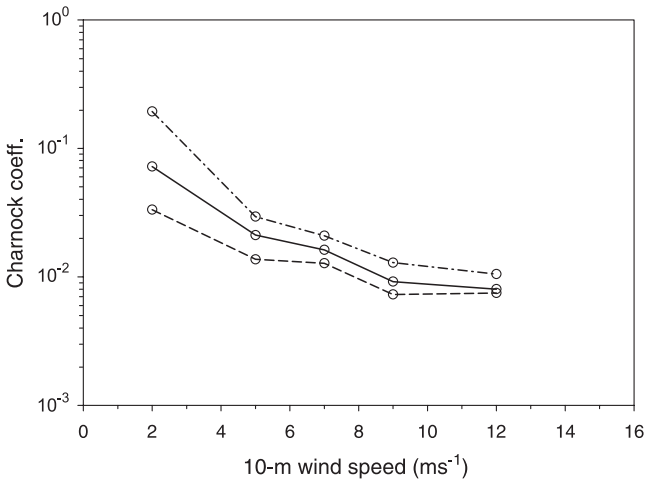


Figure 4. Dependence of the Charnock coefficient on wind speed for the RASEX data set for logarithmic averaging (solid line), linear averaging (dash-dotted line) and logarithmic average with inclusion of the smooth flow term (dashed line).

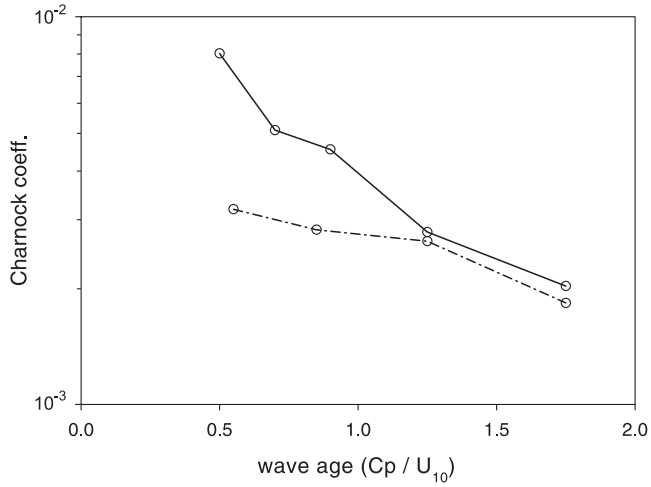


Figure 5. Dependence of the Charnock coefficient on wave age for the NPS Duck data (solid line) and the Östergarnsholm data (dash-dotted line).

[41] For the Östergarnsholm data, wind following swell with near-zero or upward momentum flux typically occurred with winds around 4 m s^{-1} [*Smedman et al.*, 1999]. For this data, the averaged Charnock coefficient is very small for winds between 4 m s^{-1} and 8 m s^{-1} (Figure 3). Here the Charnock coefficient is defined without the smooth flow term and is based on winds transformed to 10-m values using Monin-Obukhov similarity theory. Again, linear averaging of the Charnock coefficient produces larger values (Figure 4).

[42] The Charnock coefficient decreases to very small values for intermediate wind speeds for the Duck and Wallops Island data sets as well (Figure 3). For the swell-influenced data sets, the Charnock coefficient increases with increasing wind speed for winds greater than about 6 m s^{-1} and approaches more traditional values only for wind speeds greater than about 10 m s^{-1}, depending on the data set (Figure 3). The formulation with constant Charnock coefficient already implies a slow increase of roughness length with increasing wind speed (section 3), but the observed roughness length increases faster than the rate predicted by constant Charnock coefficient.

[43] After eliminating weak wind conditions, the Charnock coefficient systematically decreases with increasing wave age (C_p/U) for the Östergarnsholm data and the NPS Duck data (Figure 5). This is consistent with the notion that the very small values of the Charnock coefficient are often related to wind-following swell. The other two data sets did not show this relationship but did not contain an adequate sample of older wave ages for full examination of the dependence of the Charnock coefficient on wave age.

[44] Is the dependence of the Charnock coefficient on wind speed related to a statistical relationship between wave age and wind speed? The increase of the Charnock coefficient with strong wind speeds is statistically due in part to a general decrease of wave age with stronger wind speeds and the decreased importance of swell at stronger wind

speeds, as given by *Oost et al.* [2002] and *Drennan et al.* [2003]. High wind events can be short term and the waves may not have time to reach near-equilibrium; that is, the phase speed of the waves remains small compared to the wind speed. Wave breaking may also play a role. For the RASEX data, the wave age does indeed systematically decrease with increasing wind speed [*Vickers and Mahrt*, 1997b]. For the data sets analyzed in this study, after excluding weak winds, the wave age also decreases with increasing wind speed. The correlation between wind speed and wave age for wind speeds greater than 6 m s^{-1} are -0.6 for NPS-Duck, -0.93 for NPS-Wallops Island, -0.45 for the Östergarnsholm data, and -0.69 for the RASEX data.

[45] The averaged Charnock coefficient is smallest for intermediate wind speeds because of the increase of the Charnock coefficient at stronger wind speeds and increase of the Charnock coefficient at weak winds. Application of the smooth flow term reduces the Charnock coefficient, particularly at weak wind speeds (Figure 4), but significant increase of the Charnock coefficient at weak winds remains. Part of the increase of the Charnock coefficient at weak winds could be due to observational and analysis difficulties for weak wind speeds [*Mahrt et al.*, 1996].

[46] From a physical point of view, the Charnock formulation should not be applied to the present data sets where swell and young seas are common. However, most regional and large-scale models normally cannot accept the complexity of wave models. The correlation between the Charnock coefficient and wind speed suggests that the wind speed might be used as a statistical surrogate for the influence of wave state, even though such a surrogate would be physically indirect and incomplete. We avoid proposing such a formulation here since its generality would be unknown and the coefficients of such a formulation would be sensitive to the treatment of outliers.

7. Other Influences

[47] This analysis did not consider the direction of the swell. For swell opposing the wind, the drag coefficient is enhanced compared to pure wind-driven seas [*Donelan et al.*, 1997]. The swell propagation is often not aligned with the wind and the stress direction may be different from the wind direction. This invalidates Monin-Obukhov similarity theory, as emphasized by *Grachev and Fairall* [2001] and the roughness length and Charnock coefficient loose physical meaning. *Rieder and Smith* [1998] pose the change of the stress with wind speed by partitioning the stress into different frequency bands and separating the wave-coherent part of the stress. They find that differences between swell and wind direction, sometimes associated with nonstationarity of the wind field, can lead to wave-induced stress (eddies coherent with the wave field) that opposes the wind-induced stress. Coastal zone winds are frequently changing in time and space due to a diurnally varying component associated with thermal land-sea contrasts and SST variations as well as coastal advective effects. We are currently investigating the influence of swell direction.

[48] Very small values of the stress also occur with strong stability [*Smedman et al.*, 1997a, 1997b]. *Plant et al.* [1998] and *Mahrt et al.* [2001a] have noted that the roughness length decreases with increasing stability. Stable stratification restricts turbulent transport to the wave surface, which can lead to further decrease of the roughness length and surface stress. As a possible result, the wave model examined by *Voorrips et al.* [1996] was found to overpredict wave growth in stable conditions. The eddy correlation data analyzed by *Mahrt* [2001a] correspond to decreasing Charnock coefficient with increasing stability. However, ultra-smooth conditions are not confined to very stable cases for the present data and stability appears to be a secondary influence.

8. Conclusions

[49] For the data sets analyzed in this study, formulations for the aerodynamic roughness length based on the Charnock relationship and wave age are dominated by spurious self-correlation. Our goal was to assess the errors resulting from application of the Charnock relationship to a wide variety of conditions, as is done in many models. Most regional and large-scale models cannot accommodate the complexity and computer time required for a wave model. To construct such an assessment, we have not removed common cases of swell or other conditions where the Charnock relationship is not expected to apply.

[50] The dominance of spurious self-correlation remains even after removing cases with short fetch, weak winds, and upward momentum flux from the sea surface. In addition, the overall behavior of the Charnock coefficient is sensitive to the treatment of numerous outliers and the method for averaging over the various records. Relationships allowing the dependence of the Charnock coefficient on wave age are still dominated by self-correlation. Inclusion of information on the significant wave height modestly increases the physical variance explained. These assessments are based on linear correlation whereas the physical relationship between variables may be nonlinear.

[51] The extreme variability of the Charnock coefficient is associated primarily with very small values, which appear to be related to wind following swell and, to a lesser extent, semi-collapsed turbulence in very stable conditions. For such conditions, the roughness length is less than the smooth flow prediction; that is, the stress is "ultra-smooth." For the RASEX data set, where swell is generally absent, ultra-smooth conditions are relatively rare. The Charnock coefficient decreases with increasing wave age, C_p/U, to values much below traditional values. For the present data sets, larger wave age more often occurs for intermediate wind speeds while younger waves more often occur for stronger wind speeds. This introduces a statistical wind-speed dependence where the Charnock coefficient is small at intermediate wind speeds and increases with increasing wind speed. The Charnock coefficient also increases at weak wind speeds. Inclusion of smooth flow effects reduces but does not eliminate this increase at weak wind speeds.

[52] The Charnock formulation should theoretically not be applied to weak wind conditions and conditions with significant influence of wave state where Monin-Obukhov similarity theory and the traditional concept of an aerodynamic roughness length break down. Nonetheless, formulations based on the Charnock coefficient will probably remain a primary parameterization for closing the surface stress in numerical models because simple alternatives do

not exist. The present data sets suggest using a smaller value of the Charnock coefficient at intermediate wind speeds compared to traditional values of the Charnock coefficient, although the generality of this behavior is not known and a quantitative parameterization is not offered. The difference between the data sets in this study underscores the danger of developing process formulations based on an individual site.

[53] **Acknowledgments.** We gratefully acknowledge the helpful comments of the reviewers, which led to substantial revision of section 6. This material is based upon work supported by grants N000149710279 and N0001409810282 from the Office of Naval Research, Marine Meteorology.

References

Andreas, E., and K. Claffey, Air-ice drag coefficients in the western Weddell Sea: I. Values deduced from profile measurements, *J. Geophys. Res.*, *100*, 4833–4843, 1995.

Barthelmie, R. J., M. S. Courtney, J. Højstrup, and P. Sanderhoff, The Vindeby Project: A description, *Rep. R-741(EN)*, Risø Natl. Lab., Roskilde, Denmark, 1994.

Brutsaert, W. H., *Evaporation Into the Atmosphere*, 299 pp., D. Reidel, Norwell, Mass., 1982.

Charnock, H., Wind stress over a water surface, *Q. J. R. Meteorol. Soc.*, *81*, 639–640, 1955.

Donelan, M. A., Air-sea interaction, in *Ocean Engineering Science*, edited by B. LeMehaute and D. M. Hanes, pp. 239–292, John Wiley, New York, 1990.

Donelan, M. A., W. Drennan, and K. Katsaros, The air-sea momentum flux in conditions of wind sea and swell, *J. Phys. Oceanogr.*, *27*, 2087–2099, 1997.

Drennan, W., H. Graber, D. Hauser, and C. Quentin, On the wave age dependence of wind stress over pure wind seas, *J. Geophys. Res.*, *108*, 8062, doi:10.1029/2000JC000715, 2003.

Dyer, A. J., A review of flux-profile relationships, *Boundary Layer Meteorol.*, *7*, 363–372, 1974.

Edson, J. B., and C. W. Fairall, Similarity relationships in the marine atmospheric surface layer for terms in the TKE and scalar variance budgets, *J. Atmos. Sci.*, *55*, 2311–2328, 1998.

Fairall, C. W., E. F. Bradley, D. P. Rogers, J. B. Edson, and G. S. Young, Bulk parameterization of air-sea fluxes for Tropical Ocean-Global Atmosphere Coupled-Ocean Atmosphere Response Experiment, *J. Geophys. Res.*, *101*, 3747–3764, 1996.

Frederickson, P. A., and K. L. Davidson, Observational buoy studies of coastal air-sea fluxes, *J. Clim.*, *16*, 593–599, 2003.

Geernaert, G. L., On modeling the wind stress direction based on thermal advection and surface waves, in *The Air-Sea Interface*, edited by M. A. Donelan, W. H. Hui, and W. J. Plant, pp. 421–429, Rosenstiel School of Mar. and Atmos. Sci., Univ. of Miami, Miami, Fla., 1996.

Grachev, A., and C. Fairall, Upward momentum transfer in the marine boundary layer, *J. Phys. Oceanogr.*, *31*, 1698–1711, 2001.

Hare, J. E., T. Hara, J. B. Edson, and J. M. Wilczak, A similarity analysis of the structure of airflow over surface waves, *J. Phys. Oceanogr.*, *27*, 1018–1037, 1997.

Højstrup, J., J. Edson, J. Hare, M. S. Courtney, and P. Sanderhoff, The RASEX 1994 experiments, *Rep. Risø-R-788*, Risø Natl. Lab., Roskilde, Denmark, 1995.

Johnson, H. K., J. Høstrup, H. J. Vested, and S. E. Larsen, On the dependence of sea surface roughness on wind waves, *J. Phys. Oceanogr.*, *28*, 1702–1716, 1998.

Maat, N., C. Kraan, and W. A. Oost, The roughness of wind waves, *Boundary Layer Meteorol.*, *54*, 89–103, 1991.

Mahrt, L., D. Vickers, J. Howell, J. Edson, J. Hare, J. Højstrup, and J. Wilczak, Sea surface drag coefficients in RASEX, *J. Geophys. Res.*, *101*, 14,327 –14,335, 1996.

Mahrt, L., D. Vickers, J. Edson, J. Sun, J. Højstrup, J. Hare, and J. Wilczak, Heat flux in the coastal zone, *Boundary Layer Meteorol.*, *86*, 421–446, 1998.

Mahrt, L., D. Vickers, J. Sun, T. Crawford, G. Crescenti, and P. Frederickson, Surface stress in offshore flow and quasi-frictional decoupling, *J. Geophys. Res.*, *106*, 20,629–20,639, 2001a.

Mahrt, L., D. Vickers, J. Edson, J. Wilczak, J. Hare, and J. Højstrup, Vertical structure of offshore flow during RASEX, *Boundary Layer Meteorol.*, *100*, 47–61, 2001b.

Mitsuyasu, H., and T. Kusaba, The effect of swell on certain air-sea interaction phenomena, in *The Air-Sea Interface*, edited by M. A. Donelan, W. H. Hui, and W. J. Plant, pp. 49–53, Rosenstiel School of Mar. and Atmos. Sci., Univ. of Miami, Miami, Fla., 1996.

Oost, W., G. Komen, C. Jacobs, and C. van Oort, New evidence for a relation between wind stress and wave age from measurements during ASGAMAGE, *Boundary Layer Meteorol.*, *103*, 409–438, 2002.

Paulson, C. A., The mathematical representation of wind speed and temperature profiles in the unstable atmospheric surface layer, *J. Appl. Meteorol.*, *9*, 857–861, 1970.

Phillips, O. M., and M. Banner, The effect of swell on the growth of wind waves, *J. Fluid Mech.*, *66*, 625–640, 1974.

Plant, W., W. Keller, V. Hesany, K. Hayes, K. Hoppel, and T. Blanc, Measurements of the marine boundary layer from an airship, *J. Atmos. Oceanic Technol.*, *15*, 1433–1458, 1998.

Rieder, K. F., and J. A. Smith, Removing wave effects from the wind stress vector, *J. Geophys. Res.*, *103*, 1363–1374, 1998.

Smedman, A.-S., M. Tjernström, and U. Hogström, The near-neutral marine atmospheric boundary layer with no surface shearing stress: A case study, *J. Atmos. Sci.*, *51*, 3399–3411, 1994.

Smedman, A.-S., H. Bergström, and B. Grisogano, Evolution of stable internal boundary layers over a cold sea, *J. Geophys. Res.*, *102*, 1091–1099, 1997a.

Smedman, A.-S., U. Hogström, and H. Bergström, The turbulence regime of a very stable marine airflow with quasi-frictional decoupling, *J. Geophys. Res.*, *102*, 21,049–21,059, 1997b.

Smedman, A., U. Högström, H. Bergström, A. Rutgersson, K. Kalma, and H. Pettersson, A case-study of air-sea interaction during swell conditions, *J. Geophys. Res.*, *104*, 25,833–25,851, 1999.

Smith, S. D., Wind stress and heat flux over the ocean in gale force winds, *J. Phys. Oceanogr.*, *10*, 709–726, 1980.

Smith, S. D., et al., Sea surface wind stress and drag coefficients: the HEXOS results, *Boundary Layer Meteorol.*, *60*, 109–142, 1992.

Smith, S. D., F. W. Dobson, and R. J. Anderson, The wind stress-sea state relationship with mixed sea and swell, in *The Air-Sea Interface*, edited by M. A. Donelan, W. H. Hui, and W. J. Plant, pp. 429–436, Rosenstiel School of Mar. and Atmos. Sci., Univ. of Miami, Miami, Fla., 1996.

Sun, J., D. Vandemark, L. Mahrt, D. Vickers, T. Crawford, and C. Vogel, Momentum transfer over the coastal zone, *J. Geophys. Res.*, *106*, 12,437–12,448, 2001.

Toba, Y., and M. Koga, A parameter describing overall conditions of wave breaking, white capping, sea-spray production and wind stress, in *Oceanic Whitecaps and their Role in Air-Sea Exchange Processes*, edited by E. C. Monahan and G. Mac Niocaill, pp. 37–47, D. Reidel, Norwell, Mass., 1986.

Vickers, D., and L. Mahrt, Quality control and flux sampling problems for tower and aircraft data, *J. Atmos. Oceanic Technol.*, *14*, 512–526, 1997a.

Vickers, D., and L. Mahrt, Fetch limited drag coefficients, *Boundary Layer Meteorol.*, *85*, 53–79, 1997b.

Vickers, D., and L. Mahrt, Observations of nondimensional shear in the coastal zone, *Q. J. R. Meteorol. Soc.*, *125*, 2685–2702, 1999.

Vickers, D., L. Mahrt, J. Sun, and T. Crawford, Structure of offshore flow, *Mon. Weather Rev.*, *129*, 1251–1258, 2001.

Voorrips, A. C., V. K. Makin, and G. J. Komen, The influence of stratification of the atmospheric boundary layer on wave growth, in *The Air-Sea Interface*, edited by M. A. Donelan, W. H. Hui, and W. J. Plant, pp. 21–26, Rosenstiel School of Mar. and Atmos. Sci., Univ. of Miami, Miami, Fla., 1996.

Wilczak, J. M., J. Edson, J. Hojstrup, and T. Hara, The budget of turbulence kinetic energy in the marine atmosphere, in *Air-Sea Exchange: Physics, Chemistry and Dynamics*, edited by G. Geernaert, pp. 153–174, Kluwer Acad., Norwell, Mass., 1999.

K. Davidson and P. Frederickson, Naval Postgraduate School, Monterey, CA 93943, USA. (davidson@nps.navy.mil; pafreder@nps.navy.mil)

L. Mahrt and D. Vickers, College of Oceanic and Atmospheric Sciences, Oregon State University, Corvallis, OR 97331, USA. (mahrt@coas.oregonstate.edu; blat@coas.oregonstate.edu)

A.-S. Smedman, Department of Meteorology, University of Uppsala, S-752 36, Uppsala, Sweden. (annsofi@big.met.uu.se)